HYBRID CONTROL OF ROBOT MANIPULATOR WITHOUT FORCE SENSOR

K. Ohishi*, M. Miyazaki, M. Fujita** and Y. Ogino****

**Department of Electrical Engineering, Nagaoka University of Technology, 1603-1 Kamitomioka-cho, Nagaoka-city, Niigata, 940-21, Japan*
***Department of Electrical Engineering, Osaka Institute of Technology, 5-16-1, Omiya, Asahi-ku, Osaka-city, 535, Japan*

Abstract. This paper proposes the new hybrid control of force and position without force sensor. The proposed hybrid control system is designed by both H^∞ acceleration controller and the force estimation system. H^∞ acceleration controller realizes a fine and robust motion control. The reaction force estimation system consists of the torque observer and the inverse dynamics calculation, and its estimated value is fed to the force control system. The experimental results in this paper illustrate the fine hybrid control of the tested three-degrees-of-freedom DD robot manipulator without force sensor.

Key Words. Force control, Robotics, Digital control, H^∞ control, Acceleration control

1. INTRODUCTION

The difficulty of force control using a force sensor signal is caused by both the rigidity of force sensor and the condition of target environment. The force control system of robot manipulator should take the rigidity and nonlinearity of force sensor into account. However, it is difficult to take account of them in the motion control of robot manipulator. Besides, when the target environment of robot manipulator has a high temperature and a large noise, the force sensor can not be mounted to the robot manipulator. In order to overcome these problems, this paper proposes the force estimation method based on the torque observer(Ohishi, 1987) and the inverse dynamics calculation(An, 1988; Craig, 1986). Its estimated value is fed to the force control system instead of the signal of force sensor.

In order to realize a robust and fast motion control, the acceleration control method based on the disturbance observer has been reported(Komada, 1990). Using this method, each joint actuator of robot manipulator is driven by an acceleration control command, and the motion control system becomes robust. This paper adopts the acceleration control method based on H^∞ control theory(Doyle, 1989; Francis, 1987). H^∞ control design method using the mixed sensitivity discusses the frequency characteristics of acceleration controller.

Using both H^∞ acceleration controller and the force estimation system, this paper proposes the new hybrid control system without force sensor.

2. HYBRID CONTROL BASED ON ACCELERATION CONTROLLER

Fig.1 shows the hybrid control system of multi-degrees-of-freedom robot manipulator using the acceleration controller. In Fig.1, the position $\boldsymbol{P}(s)$, the velocity $\dot{\boldsymbol{P}}(s)$ and the acceleration $\ddot{\boldsymbol{P}}(s)$ of Cartesian Axis Space are defined by the position $\boldsymbol{\theta}$, the velocity $\boldsymbol{\omega}$ and the acceleration $\dot{\boldsymbol{\omega}}$ of each Joint Axis Space, as shown in eq.(1), eq.(2) and eq.(3) respectively. Here, $T(\boldsymbol{\theta}(s))$ is the transformation matrix from the position $\boldsymbol{P}(s)$ of Cartesian Axis Space to the position $\boldsymbol{\theta}(s)$ of each Joint Axis Space. $\boldsymbol{J}(s)$ is the Jacobian matrix. Therefore, the transformation from the acceleration control command $\ddot{\boldsymbol{P}}^{cmd}(s)$ of Cartesian Axis Space to the acceleration control command $\dot{\omega}^{cmd}$ of each Joint Axis Space is defined by eq.(4).

$$\boldsymbol{P} = \boldsymbol{T}(\boldsymbol{\theta}) \tag{1}$$

$$\dot{\boldsymbol{P}} = \boldsymbol{J}\boldsymbol{\omega} \tag{2}$$

$$\ddot{\boldsymbol{P}} = \boldsymbol{J}\dot{\boldsymbol{\omega}} + \dot{\boldsymbol{J}}\boldsymbol{\omega} \tag{3}$$

$$\dot{\omega}^{cmd} = \boldsymbol{J}^{-1}\ddot{\boldsymbol{P}}^{cmd} - \boldsymbol{J}^{-1}\dot{\boldsymbol{J}}\boldsymbol{\omega} \tag{4}$$

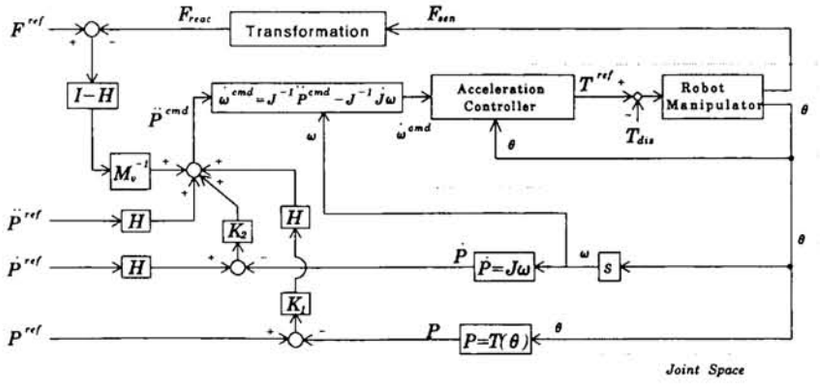

Fig.1. Block diagram of hybrid control system of position and force

The force control system is constructed as shown in the upper part of Fig.1. Similarly, the position control system is constructed as shown in the lower part. $\boldsymbol{M}_v$ is the virtual mass in case of force control. $\boldsymbol{H}$ is the choice matrix between the position control and the force control. When the diagonal elements of $\boldsymbol{H}$ are unity, this hybrid control system becomes the position control system. On the other hand, when the diagonal elements of $\boldsymbol{H}$ are zero, it becomes the force control system. $\boldsymbol{K}_1$ and $\boldsymbol{K}_2$ are the state feedback gain matrix for the position control respectively. In the force control, $\boldsymbol{K}_2$ is also the feedback gain to suppress the vibration between the target environment and the robot manipulator. As this hybrid control is regulated by the acceleration control command $\ddot{\boldsymbol{P}}^{cmd}(s)$, its control law has no inverse dynamics calculation. Therefore, the motion control law becomes simple.

Fig.2 shows the structure of acceleration controller (Komada, 1990; Ohishi, 1992). For the purpose of realizing a fast and fine robot motion control, each joint actuator of robot manipulator should be driven by the acceleration control command. Each joint actuator has the dynamical nonlinearity caused by both the mechanical parameter variation and the several force disturbances. The acceleration controller has no mechanical system parameter and force disturbance as shown in Fig.2.

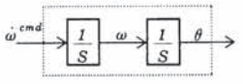

Fig.2. Acceleration controller

H^∞ control theory can design the robust acceleration controller systematically. Fig.3 shows the augmented system for H^∞ control design method using the mixed sensitivity. $K(s)$ is the state feedback element which is designed by the H^∞ design method. $P(s)$ represents the dynamics of actual actuator of robot manipulator. T_{dis} represents the force disturbance of $P(s)$. d is the disturbance input of the augmented system because this paper pays attention to the output influence of the force disturbance T_{dis}. The weighting functions, such as $W_1(s)$ and $W_2(s)$, reflect the requirement on disturbance rejection and robustness respectively.

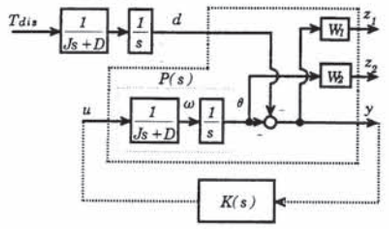

Fig.3. Augmented system for mixed sensitivity H^∞ control design method

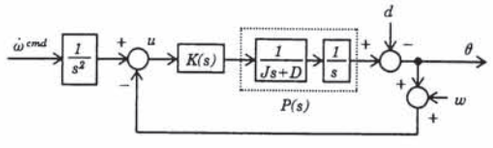

Fig.4. Schematic diagram of H^∞ acceleration controller

$$\frac{\theta}{\dot{\omega}^{cmd}} = \frac{P(s)K(s)}{1+P(s)K(s)} \cdot \frac{1}{s^2} = T(s) \cdot \frac{1}{s^2} \quad (5)$$

$$\frac{\theta}{d} = \frac{1}{1+P(s)K(s)} = S(s) \quad (6)$$

When $K(s)$ is determined by H^∞ control design method, the robust acceleration controller is constructed as shown in Fig.4. Here, w is the sensor noise input. Each transfer function is represented as shown in eq.(5) and eq.(6). Eq.(5) points out that the response characteristics of this acceleration controller is determined by the complementary sensitivity function $T(s)$. The complementary function $T(s)$ is determined by the frequency characteristics of the sensor noise influence. Moreover, on the basis of the characteristics of sensitivity function $S(s)$, this acceleration controller suppresses the effects of both mechanical parameter variation and force disturbance. This paper calls it H^∞ acceleration controller, which is a robust acceleration controller.

3. FORCE ESTIMATION SYSTEM

In case of motion control of multi-degrees-of-freedom robot manipulator, the actuator of each joint has the force disturbance $\boldsymbol{T}_{dis}$, which includes the reaction force $\boldsymbol{T}_{reac}$ from target environment, the viscosity friction force $\boldsymbol{D\omega}$ and the coulomb friction force $\boldsymbol{F}$, the interactive force $\boldsymbol{T}_{int}$, the gravity force $\boldsymbol{T}_g$ and the non-linear inertia term $\Delta\boldsymbol{J}\dot{\boldsymbol{\omega}}$, as shown in eq.(7). From eq.(7), the reaction force $\boldsymbol{T}_{reac}$ of each Joint Axis Space is shown by eq.(8). Hence, when the values of $\boldsymbol{T}_{dis}$, $\boldsymbol{D\omega}$, $\boldsymbol{F}$, $\boldsymbol{T}_{int}$, $\boldsymbol{T}_g$ and $\Delta\boldsymbol{J}\dot{\boldsymbol{\omega}}$ are identified, the reaction force $\boldsymbol{T}_{reac}$ is estimated on the basis of the inverse dynamics calculation using eq.(8).

$$\boldsymbol{T}_{dis} = \boldsymbol{T}_{int} + \boldsymbol{T}_g + \boldsymbol{T}_{reac} + \boldsymbol{D\omega} + \boldsymbol{F} + \boldsymbol{T}_l + \Delta\boldsymbol{J}\dot{\boldsymbol{\omega}} \quad (7)$$

$$\boldsymbol{T}_{reac} = \boldsymbol{T}_{dis} - \boldsymbol{T}_{int} - \boldsymbol{T}_g - \boldsymbol{D\omega} - \boldsymbol{F} - \boldsymbol{T}_l - \Delta\boldsymbol{J}\dot{\boldsymbol{\omega}} \quad (8)$$

The force disturbance T_{dis} is identified by using the torque observer as shown in Fig.5. $H(s)$ is the product of the low-pass filter $F(s)$ and the nominal actuator model $P_m(s)$, which are represented as shown in eq.(9), eq.(10) and eq.(11) respectively. The natural frequency ω_n of $F(s)$ determines the frequency characteristics of torque observer. This torque observer estimates the force disturbance T_{dis} within the frequency band of $F(s)$.

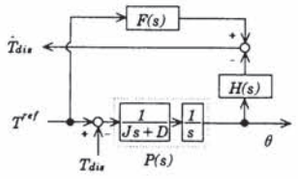

Fig.5. Block diagram of torque observer

$$H(s) = F(s)P_m(s) \quad (9)$$

$$F(s) = \frac{{\omega_n}^2}{s^2 + 2\omega_n s + {\omega_n}^2} \quad (10)$$

$$P_m(s) = \frac{1}{J_n s} \cdot \frac{1}{s} \quad (11)$$

Next, for the purpose of identifying the values of $\boldsymbol{D\omega}$, $\boldsymbol{F}$, $\boldsymbol{T}_{int}$, $\boldsymbol{T}_g$ and $\Delta\boldsymbol{J}\dot{\boldsymbol{\omega}}$, this paper describes the motion experiment of each joint of robot manipulator. Generally, the dynamic equation of robot manipulator in Joint Axis Space is represented as shown in eq.(12). In eq.(12), τ is the input torque matrix, and $\boldsymbol{M}$ is the inertia matrix.

$$\tau = \boldsymbol{M}\dot{\boldsymbol{\omega}} + \boldsymbol{T}_{int} + \boldsymbol{T}_g + \boldsymbol{D\omega} + \boldsymbol{F} \quad (12)$$

First, the constant velocity motion experiment of robot manipulator is carried out. On condition that the joint acceleration is zero, i.e. $\dot{\boldsymbol{\omega}} = 0$, eq.(12) is equal to eq.(13). Therefore, the gravity force $\boldsymbol{T}_g$, the viscosity friction force $\boldsymbol{D\omega}$ and the coulomb friction force $\boldsymbol{F}$ of each joint are identified from

the data of the position θ, the constant velocity ω, the input force τ and the estimated force disturbance T_{dis}, of the torque observer.

$$\tau = T_g + D\omega + F \tag{13}$$

Second, using the identified values of T_g, $D\omega$ and F in the first experiment, the interactive force T_{int} and the non-linear inertia term $\Delta J\dot{\omega}$ in each joint are identified from the estimated force disturbance $\hat{T}_{dis}$ to the step change of the constant velocity ω.

As a result, the reaction force T_{reac} is estimated on the basis of the inverse dynamics calculation using eq.(8). Hence, the proposed force estimation system is constructed by both the torque observer and the inverse dynamics calculation as shown in Fig.6.

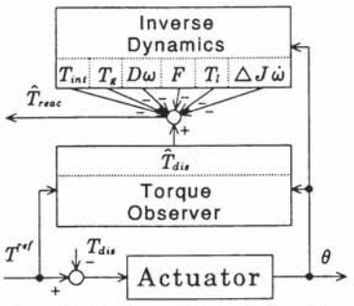

Fig.6. Schematic diagram of force estimation system

4. HYBRID CONTROL WITHOUT FORCE SENSOR

The hybrid control system as shown in Fig.1 must have the information of both the position θ and the reaction force F_{reac}. The force control system of robot manipulator should take the rigidity and nonlinearity of force sensor into account. However, it is difficult to take account of them in the motion control of robot manipulator. Besides, when the target environment of robot manipulator has a high temperature and a large noise, the force sensor can not be mounted to the robot manipulator. In order to overcome these problems, this paper proposes the new hybrid control system without force sensor.

The proposed hybrid control system is designed by both the H^{∞} acceleration controller and the force estimation system, as shown in Fig.7. The estimated reaction force $\hat{T}_{reac}$ is the data of Joint Axis Space. This value is transformed into the data of Cartesian Axis Space by using eq.(14). Here, J^T is the transposed matrix of Jacobian matrix.

$$\hat{F}_{reac} = \left(J^T\right)^{-1} \hat{T}_{reac} \tag{14}$$

5. EXPERIMENTAL RESULTS

The tested three-degrees-of-freedom DD robot manipulator is shown in Fig.8. Here, the dynamical force equation of tested robot manipulator is represented as shown in eq.(15). In eq.(15), $M(\theta)$ is the inertia matrix, $B(\theta)$ is the Coriolis force matrix and $C(\theta)$ is the centrifugal force matrix. Fig.9 represents the friction models of each joint of the tested robot manipulator respectively. They are identified from the data of the constant velocity motion experiment. In this case, the dynamical force equation of tested robot manipulator is represented as shown in eq.(16). Therefore, each gravity force T_g is also identified by the same motion experiment as shown in Table.1.

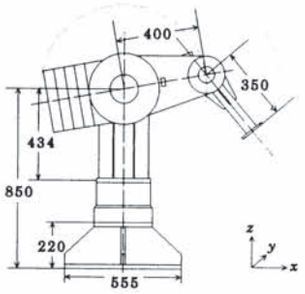

(a) Schematic diagram of tested three-degrees-of-freedom DD robot manipulator

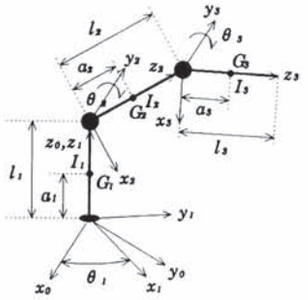

l_i : length of link i

a_i : length between joint i and the center of gravity of link i

m_i : mass of link i

$I_i = \begin{bmatrix} I_{xi} & 0 & 0 \\ 0 & I_{yi} & 0 \\ 0 & 0 & I_{zi} \end{bmatrix}$: moment of inertia of link i about the center of gravity of link i

(b) Parameter of tested DD robot manipulator

Fig.8. Tested 3-degrees-of-freedom DD robot manipulator

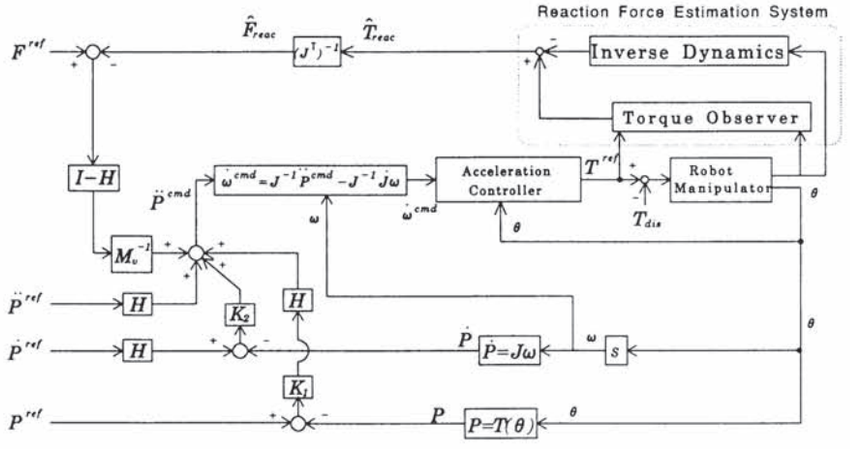

Fig.7. Hybrid control system of position and force without force sensor

$$\tau = \boldsymbol{M}(\theta)\dot{\omega} + \underbrace{\boldsymbol{B}(\theta)[\omega\omega] + \boldsymbol{C}(\theta)\left[\omega^2\right]}_{\Rightarrow \boldsymbol{T}_{int}} + \boldsymbol{T}_g(\theta) + \boldsymbol{D}\omega + \boldsymbol{F} \tag{15}$$

$$\boldsymbol{M}(\theta) = \begin{bmatrix} J_{z_1} + J_{x_2}s_2^2 + J_{x_3}s_{23}^2 + 2r_3l_2s_2s_{23} & 0 & 0 \\ 0 & J_{y_2} + J_{y_3} + 2r_3l_2c_3 & J_{y_3} + r_3l_2c_3 \\ 0 & J_{y_3} + r_3l_2c_3 & J_{y_3} \end{bmatrix}$$

$$\boldsymbol{B}(\theta) = \begin{bmatrix} 2J_{x_2}s_2c_2 + 2J_{x_3}s_{23}c_{23} + 2r_3l_2s_{(2\theta_2+\theta_3)} & 0 & 0 \\ 0 & 0 & -2r_3l_2s_3 \\ 0 & 2J_{x_3}s_{23}c_{23} - 2r_3l_2s_2c_{23} & 0 \end{bmatrix}$$

$$\boldsymbol{C}(\theta) = \begin{bmatrix} 0 & 0 & 0 \\ -J_{x_2}s_2c_2 - J_{x_3}s_{23}c_{23} - r_3l_2s_{(2\theta_2+\theta_3)} & 0 & r_3l_2s_3 \\ -J_{x_3}s_{23}c_{23} - r_3l_2s_2c_{23} & -r_3l_2\omega_3^2s_3 & 0 \end{bmatrix}$$

$$\boldsymbol{T}_g(\theta) = \begin{bmatrix} 0 \\ -r_2gs_2 - r_3gs_{23} \\ -r_3gs_{23} \end{bmatrix}$$

$$\boldsymbol{D} = \begin{bmatrix} D_1 & 0 & 0 \\ 0 & D_2 & 0 \\ 0 & 0 & D_3 \end{bmatrix}$$

$$\boldsymbol{F} = \begin{bmatrix} D_{frc1}\mathrm{sgn}\ \omega_1 \\ D_{frc2}\mathrm{sgn}\ \omega_2 \\ D_{frc3}\mathrm{sgn}\ \omega_3 \end{bmatrix}$$

$$[\omega\omega] = \begin{bmatrix} \omega_1\omega_2 \\ \omega_2\omega_3 \\ \omega_3\omega_1 \end{bmatrix}$$

$$\left[\omega^2\right] = \begin{bmatrix} \omega_1^2 \\ \omega_2^2 \\ \omega_3^2 \end{bmatrix}$$

$$\begin{aligned} s_2 &= \sin\ \theta_2,\ s_{23} = \sin(\theta_2 + \theta_3) \\ c_2 &= \cos\ \theta_2,\ c_{23} = \cos(\theta_2 + \theta_3) \\ s_{(2\theta_2+\theta_3)} &= \sin(2\theta_2 + \theta_3) \end{aligned}$$

$$\begin{aligned} J_{z_1} &= I_{z_1} + I_{z_2} + I_{z_3} \\ J_{x_2} &= I_{x_2} - I_{z_2} + m_2a_2^2 + m_3l_2^2 \\ J_{y_2} &= I_{y_2} + m_2a_2^2 + m_3l_2^2 \\ J_{x_3} &= I_{x_3} - I_{z_3} + m_3a_3^2 \\ J_{y_3} &= I_{y_3} + m_3a_3^2 \\ r_2 &= m_2a_2 + m_3l_2 \\ r_3 &= m_3a_3 \end{aligned}$$

$$\tau = \boldsymbol{T}_g + \boldsymbol{D}\omega + \boldsymbol{F} \tag{16}$$

$$\Downarrow$$

$$\begin{cases} \tau_1 = D_1\omega_1 + D_{frc1}\mathrm{sgn}\ \omega_1 \\ \tau_2 = -r_2gs_2 - r_3gs_{23} + D_2\omega_2 + D_{frc2}\mathrm{sgn}\ \omega_2 \\ \tau_3 = -r_3gs_{23} + D_3\omega_3 + D_{frc3}\mathrm{sgn}\ \omega_3 \end{cases}$$

Table 1. Gravity parameter

Gravity parameter	Value [kgm]
r_2	0.796
r_3	0.318

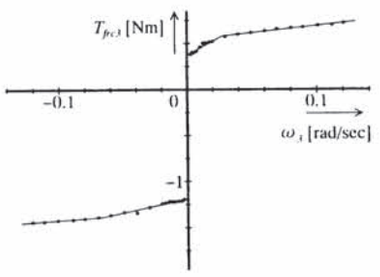

(a) 3rd axis

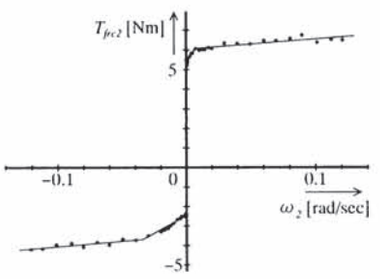

(b) 2nd axis

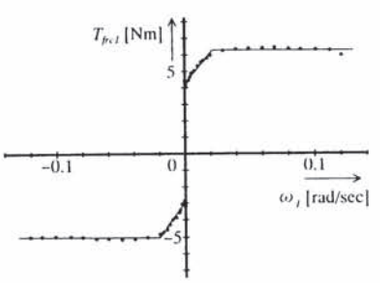

(c) 1st axis

Fig.9. Friction model

The total system of the proposed hybrid control is constructed by the software algorithm of DSP μPD77230 as shown in Fig.10, whose sampling time is 1[msec]. In the tested H^∞ acceleration controller of each joint, the frequency characteristics of sensitivity function $S(s)$ and complementary sensitivity function $T(s)$ are represented as shown in Fig.11. The natural frequency ω_n of $F(s)$ of the tested torque observer is 100[rad/sec]. Both values of the feedback constant $\boldsymbol{K}_1$ and $\boldsymbol{K}_2$ are 10.

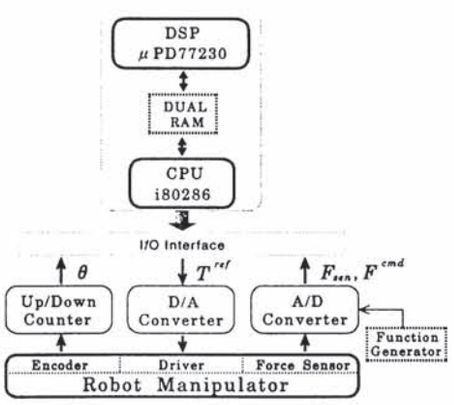

Fig.10. Hardware system of tested DD robot manipulator

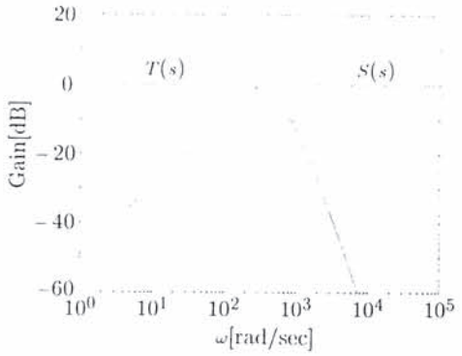

Fig.11. Frequency characteristics of tested H^∞ acceleration controller

The experimental results of the proposed hybrid control are represented as shown in Fig.12. Fig.13 shows the tested pose of robot manipulator in this case. These experimental results show the comparison between the hybrid control system with force sensor and the proposed hybrid control system without force sensor. The direction of force control is X Axis. The force reference $\boldsymbol{F}^{ref}$ is the step-like wave form whose frequency is 1[Hz]. The direction of position control is Y and Z Axis. The position reference $\boldsymbol{P}^{ref}$ is the straight line wave form of Y Axis direction whose velocity is 0.02 [m/sec]. Z Axis direction is regulated to the constant position.

In the proposed hybrid control system, the force control to X Axis direction is stable, and it is almost tracking to the force reference $\boldsymbol{F}^{ref}$. The position control to Y Axis is accurately tracking to the position reference $\boldsymbol{P}^{ref}$. The responses of the proposed hybrid control without force sensor well coincide with them of the hybrid control with force sensor.

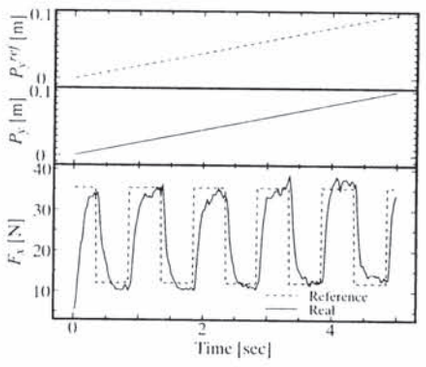

(1) With force sensor

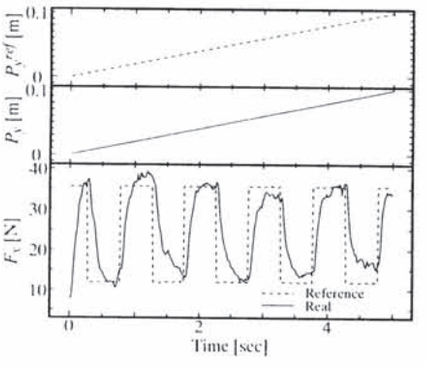

(2) Without force sensor

Fig.12. Experimental results of hybrid control of position

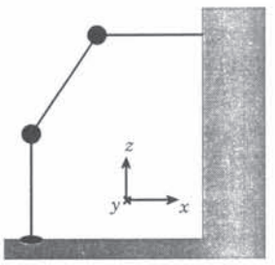

Fig.13. Tested pose of robot manipulator

6. CONCLUSION

This paper proposes the new hybrid control system without force sensor. The proposed hybrid control system has H^∞ acceleration controller and the force estimation system. The robust acceleration controller is systematically designed on the basis of the mixed sensitivity H^∞ design method. The force estimation system is constructed by both the torque observer and the inverse dynamics calculation. The experimental results confirm that the proposed hybrid control system well regulates both the force to the target environment and the position of robot manipulator.

7. REFERENCES

Ohishi, K., et al. (1987). Microprocessor-Controlled DC Motor for Load-Insensitive Position Servo System. *IEEE. Trans. on Industrial Electronics*, Vol. 34, No. 1, pp. 44–49.

An, C.H., et al. (1988). Model-Based Control of a Robot Manipulator. *The MIT Press.*

Craig, J.J. (1986). Introduction to Robotics : Mechanics & Control. *Addison-Wesley Publishing Company.*

Komada, S., et al. (1990). Force Feedback Control of Robot Manipulator by the Acceleration Tracing Orientation Method. *IEEE. Trans. on Industrial Electronics*, Vol. 37, No. 1 pp. 6–12.

Doyle, J.C., et al. (1989). State-Space Solutions to Standard H_2 and H_∞ Control Problems. *IEEE. Trans. on Automatic Control*, Vol. 34, pp. 831–847.

Francis, B.A. (1987). A Course in H^∞ Control Theory. *Springer-Verlag.*

Ohishi, K., et al. (1992). Force Control without Force Sensor Based on Mixed Sensitivity H^∞ Design Method. *Proc. of 1992 IEEE. Int. Conf. on Robotics and Automation*, Vol. 2, pp. 1356–1361.

Appendix

Identification of Inertia Matrix $\boldsymbol{M}(\boldsymbol{\theta})$, Coriolis Force Matrix $\boldsymbol{B}(\boldsymbol{\theta})$ and Centrifugal Force Matrix $\boldsymbol{C}(\boldsymbol{\theta})$

The torque observer estimates the force disturbance T_{ds}, within the frequency band of $F(s)$, as shown in eq.(17). If the force estimation system only takes account of the force disturbance T_{ds}, within the natural frequency ω_n of $F(s)$, $F(s)$ can be treated as the unity function. In this case, eq.(17) becomes eq.(18) nearly. Eq.(18) is transformed into eq.(19). When the actual value of inertia moment J is not that of the nominal inertia moment J_n, the value of $\hat{T}_{ds}$ in eq.(18) has the effect of parameter mismatching of inertia moment. In other words, when the value of T_{ds} has no its effect, the nominal inertia moment J_n of torque observer is regarded as the actual inertia moment J.

$$\hat{T}_{dis} = F(s)\{(J - J_n)\dot{\omega} + T_{dis}\} \quad (17)$$

$$\hat{T}_{dis} \simeq (J - J_n)\dot{\omega} + T_{dis} \quad (18)$$

$$\hat{T}_{dis} - T_{dis} = (J - J_n)\dot{\omega} \quad (19)$$

In the tested robot manipulator, the force disturbance T_{dis} of the third axis is represented as shown in eq.(20) in case that the nominal inertia J_n is the actual value. Substituting eq.(20) for eq.(19), the relation between the estimated value of $\hat{T}_{dis}$ and the dynamical motion equation is represented as shown in eq.(21). In eq.(21), the values of $\boldsymbol{T}_g$, $\boldsymbol{D}$ and $\boldsymbol{F}$ are identified by the former constant velocity motion experiment respectively. Fig.14 shows the response of torque observer to the step change of the velocity ω of the third axis. When this step response has no $T_{dis,peak}$, the nominal inertia moment J_n of torque observer has the actual value. Therefore, the inertia moment J_{y3} of the third axis can be identified from each value of $\hat{T}_{dis}$, T_g, D and F to the step change of the velocity ω.

$$T_{dis3} = -r_3 g s_{23} + D_3\omega_3 + D_{frc3}\mathrm{sgn}\ \omega_3 \quad (20)$$

$$\underbrace{\hat{T}_{dis3} + r_3 g s_{23} - D_3\omega_3 - D_{frc3}\mathrm{sgn}\ \omega_3}_{e_{rr}} = (J_3 - J_{y3})\dot{\omega}_3 \quad (21)$$

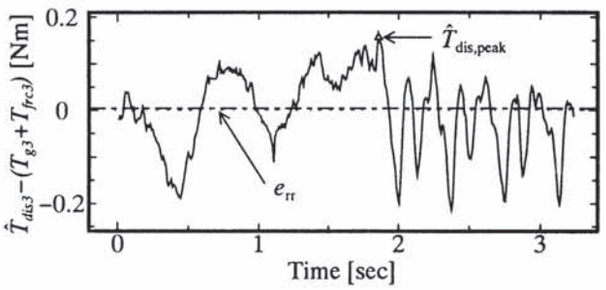

Fig.14. Velocity step response

Fig.15 shows the identification process of the inertia moment J_{y3} of the third axis. In Fig.15, each triangle plot means the magnitude of $T_{dis,peak}$ on condition that the several values of inertia moment are substituted for the nominal inertia moment J_n of torque observer. The cross point of the err-line and the triangle-plot-line means the actual value of the inertia moment J_{y3}.

Similarly, the actual values of the inertia moment J_{y2}, J_{z1}, J_{x2} and J_{x3} are identified by this step velocity response. Hence, the inertia matrix $\boldsymbol{M}(\boldsymbol{\theta})$ of the tested robot manipulator is determined by these inertia moments, the gravity force parameters and each link length, as shown in eq.(15). Moreover, the Coriolis force matrix $\boldsymbol{B}(\boldsymbol{\theta})$ and the centrifugal force matrix $\boldsymbol{C}(\boldsymbol{\theta})$ are also determined by these inertia moments, the gravity force parameters and each link length.

As a results, all parameters of the dynamical motion equation of robot manipulator are identified by using the torque observer. This identification strategy needs not have the force sensor. Therefore, the proposed hybrid control system is designed without force sensor, and is constructed without it, too.

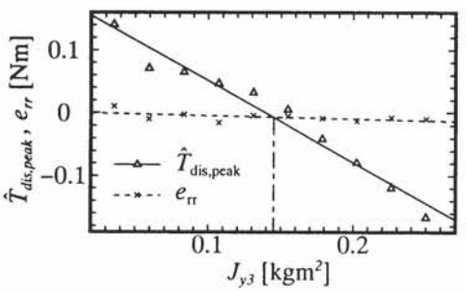

Fig.15. Experimental results of inertia